Proceedings of the Sixteenth International Conference on
Computational Structures Technology
Edited by: P. Iványi, J. Kruis and B.H.V. Topping
Civil-Comp Conferences, Volume 14, Paper 7.1
Civil-Comp Press, Edinburgh, United Kingdom, 2026
ISSN: 2753-3239, doi: 10.4203/ccc.14.7.1

Buckling of Domes From Functionally Graded Auxetics

J. Blachut[1], M. D. White[1] and D. Sala[2]

[1]Department of Mechanical and Aerospace Engineering, University of Liverpool, United Kingdom
[2]Faculty of Management, AGH - University of Science and Technology, Krakow, Poland

Abstract

Metallic auxetics are likely to be porous and until recently it would be impossible to have several layers of distinctly different, yet auxetic, layers to be merged. A very recent development of an auxetic substrate film capable of bonding different porous layers, made it possible to research gradually changing material properties through the wall thickness in shell structures. This paper studies the effect of functionally graded layers on the buckling of externally pressurised domes. Six-layer auxetic shell has larger buckling pressures for dominant presence of auxetic material. The opposite happens when the content of auxetic is diminished. There is virtually no effective stress jump between internal layers. The stress jump between top and bottom surfaces in 2-layer shell are seven times larger than in six-layers with functionally graded Young's modulus and Poisson's ratio. It is also noted that there is no difference between apex load deflections curves between 2-layer (50 percent steel and 50 percent auxetic) and graded six-layer dome. All comparisons are made for geometrically identical shells with elastic perfectly plastic modelling of material. The yield point was kept constant and was not subject of grading through the wall thickness.

Keywords: auxetic shell, functionally graded material, buckling, elastic-plastic, external pressure, dome.

1 Introduction

Buckling of externally pressurized domes onto cylindrical shells has been the subject of research effort for many decades, and it is continuing, e.g., references [1-4]. In engineering practice, despite above, the design of metallic, hybrid, carbon fiber plastic, etc. domes still utilizes design codes, e.g., references [5-8]. The code-based approach is due to the wide use of these shells right across underwater, on land and in space applications. The existing design codes cover a string of shapes, i.e., hemispheres, spherical caps, torispheres and ellipsoids. Arrival of 'wonder material', i.e., carbon nano tubes and carbon nanoplates triggered fresh interest in shells utilizing them, e.g., references [9,10].

The most recent addition to the new and exciting materials is associated with metamaterials. Auxetic metamaterials are a unique class of materials with a negative Poisson's ratio, and a wide array of functionalities. The current contribution provides a fresh look at multilayer hybrid auxetic dome through the optics of functionally graded materials approach. As an illustration, torispherical shells are taken in this study as a specific geometry of domed closure onto cylindrical shell.

2 Summary of recent developments regarding externally pressurised domes

2.1 Buckling behaviour of externally pressurized domes

Buckling of externally pressurized shells has a long history, and it also applies to externally pressurized domes having various shapes of their generator.

As an example, consider steel torispheres of one layer with wall thickness, t, with its geometry defined by the ratio: $(R_s/D) = 1.0$, $(D/t) = 1000$, and $(r/D) = 0.20$ as sketched in figure 1a. Assume that the torisphere is fully clamped at its equatorial plane, and its material properties are given by: Young's modulus, E = 207.0 GPa with the yield point of material, σ_{yp}= 300 MPa. In what follows, a brief illustration is given how this kind of shells behave under quasi-static incremental uniform external pressure, p. Two pieces of software are used to estimate the load carrying capacity, i.e., bifurcation buckling pressure, and/or collapse pressure. They are Bosor5 and Abaqus, references [11,12]. It is assumed that numerical analyses are based on elastic perfectly plastic modelling of material coupled with geometrical nonlinearities.

Under incremental external pressure the above torisphere will deform as it is illustrated in figure 2a, where it is seen that most of the spherical cap remains in a membrane state. Bending occurs at the cap-knuckle junction. At load called bifurcation buckling pressure, the shell suddenly snaps into asymmetric mode with n = 15 circumferential waves – as illustrated in figure 2b. Comparisons of predictions given by Abaqus and Bosor5, and modelling methodology, are available in reference [13]. It is seen there that predictions of magnitudes of various failure modes given by both codes are the same. Also, the eigenmode given by both codes is the same, i.e., n = 15 waves in hoop direction. It has to be said that in experimentation one rarely sees bifurcation mode of failure. One example where the asymmetric mode (bifurcation), was captured/photographed for domes subjected to vacuum is documented in reference [14]. Once buckling pressure is reached (be it bifurcation or collapse), there is no residual strength and the shell is destroyed. Further information on buckling/collapse of domes subjected to external pressure (including experimental data), can be found in references [1,2].

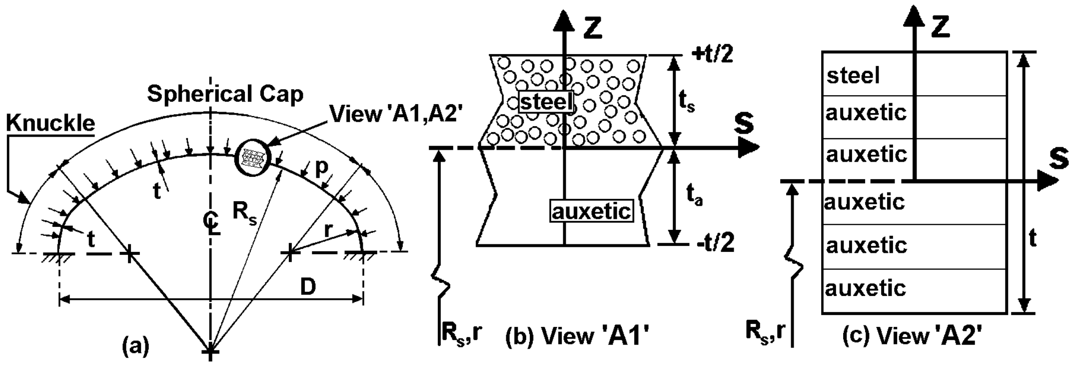

Figure 1: Geometry of torisphere and two types of wall thickness composition.

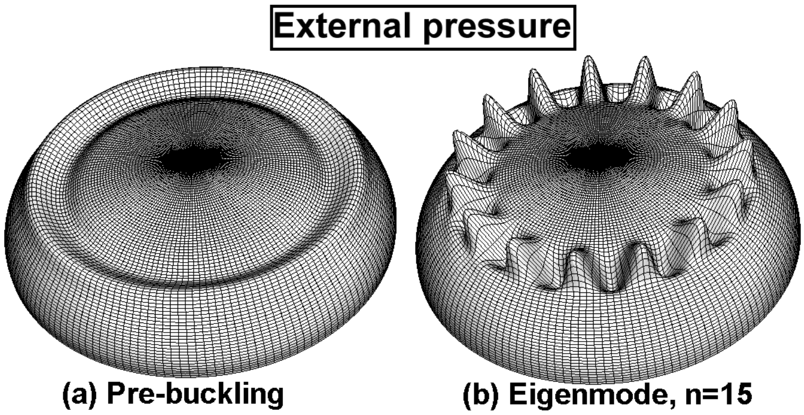

Figure 2: Shapes just prior to buckling (pre-buckling, Fig. 2a), and shape at bifurcation buckling (Fig. 2b).

2.2 Buckling behaviour of externally pressurized auxetic domes

A subset of metamaterials is known as auxetics. They possess a Negative Poisson's Ratio, NPR. Materials and structures that demonstrate auxetic behaviour, and whose base material are metal - are defined as metallic auxetics and auxetic structures. There are very few auxetic, metallic structural elements which found the way out of laboratories. They are mostly confined to plates and cylinders, e.g., references [15-18]. Several numerical studies into buckling behaviour of: (i) one layer auxetic, (ii) three-layer sandwich (steel-auxetic-steel), and (iii) two-layer (steel-auxetic) torispheres were studied in references [19-22]. Analyses included elastic perfectly plastic modelling of both steel and auxetic layers. Typical values were assumed for mild steel, i.e., Young's modulus, E_s = 207.0 GPa, the yield point of material, σ_{yp} = (300.0 or 414.0) MPa. Young's modulus of auxetic layer, E_a, was varied between 207.0 GPa and 20.7 GPa. The Poisson's ratio for steel was always kept at, $\upsilon_s = +0.30$, and for the auxetic layer it varied between, $\upsilon_a = +0.30$ and $\upsilon_a = -0.90$. The wall thickness of steel layer, t_s, and that of auxetic layer, t_a, were chosen in such a way that $t = t_a + t_s$, with the ratio, (D/t) taken between 250 and 2000. For each case the ratio, (t_a/t_s), varied between 0.0 (steel only) and 1.0 (auxetic only). Figure 3 depicts results

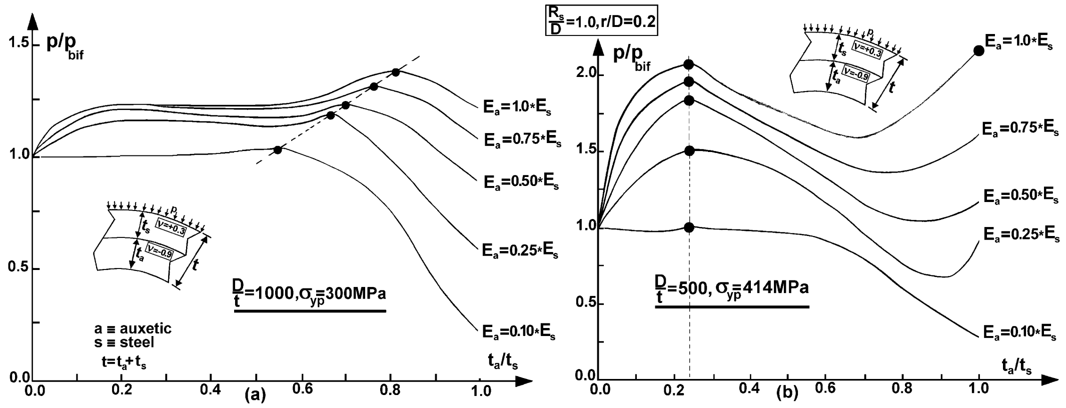

Figure 3: Buckling of two-layer torispheres with different wall thicknesses of steel and auxetic.

for two-layer torispheres (D/t = 500 and 1000, r/D = 0.2), subjected to external pressure. It is seen here that the magnitude of buckling pressure has a local maximum between configurations (steel-layer, only; $t_a/t_s = 0.0$) and (auxetic-layer, only; $t_a/t_s = 1.0$).

One of issues in analysis/design of externally pressurized domes is sensitivity of their buckling pressure (be it axisymmetric collapse or asymmetric bifurcation), to unavoidable shape imperfections, and manufacturing defects, reference [22]. Single-layer, and two-layer shells both with global (eigen-mode affine), and local (Force-Induced-Dents) imperfections are studied in this reference. Manufacturing defects in the form of local wall thickness are also analyzed. Figure 4 shows the influence of auxetic's Young's modulus on the magnitude of buckling pressure in two-layer shell (steel layer on outside with $\upsilon_s = +0.30$, and the inner auxetic layer with variable, υ_a). Two values were taken for the Young's values of auxetic layer, i.e., E_a, = 207.0 GPa and 20.7GPa. At $\upsilon_a = +0.30$ both shells bifurcate with 0.143 MPa (15) and 0.055MPa (18), respectfully. This gives the ratio of buckling pressure as 0.143/0.055 = 2.60. In the first case the buckling strength increases to 0.176 MPa at $\upsilon_a = -0.90$ giving the ratio 0.176/0.143 = 1.23. In the second case one has the increase from 0.055 MPa to 0.148 MPa, i.e., 0.148/0.055 = 2.69. This is a substantial increase and significantly different from the result obtained for E_a = 207.0 GPa.

It is worth noting here that the auxetic layer is likely to be porous. Until now it was difficult to imagine how to place auxetic layers having different properties on top of each other. Their inherent porosity presents therefore challenges in practical applications. Filling the inherent perforations while preserving their unique auxeticity is difficult because it demands the seamless integration of components that have highly distinct mechanical characteristics. A seamless auxetic substrate film capable of achieving a negative Poisson's ratio of -1, the theoretical limit of isotropic materials has been reported in reference [23]. This breakthrough was realized by incorporating a highly rigid auxetic structure reinforced by glass-fabric, with surface flattening soft elastomers. Using the developed auxetic film it was demonstrated that it was capable of 25% stretching without performance degradation.

This 'thin coupling' auxetic film which could bond auxetic layers possessing different properties has motivated the current study. Through the thickness material

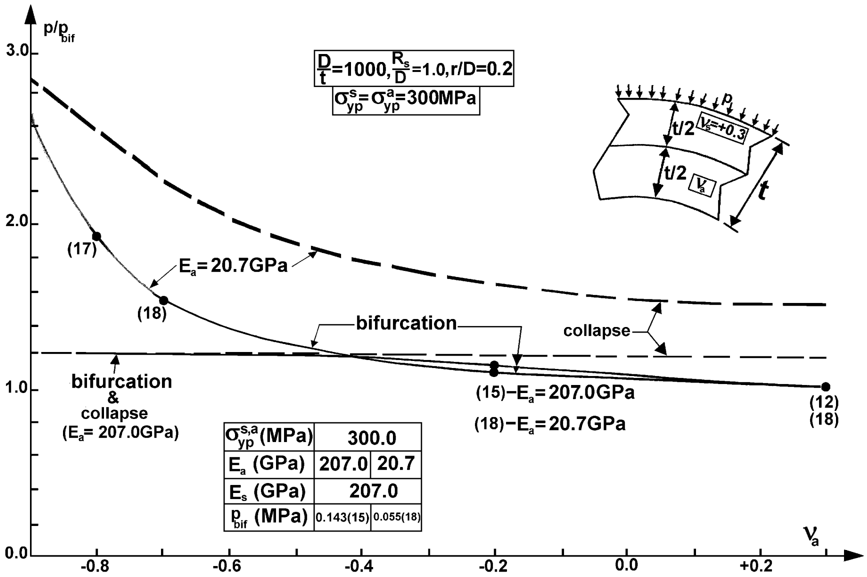

Figure 4: Influence of auxetic's layer Young's, E_a = 20.7 GPa, modulus on bifurcation and collapse. Comparison with results for E_a = 207.0 GPa . In both cases two-layer torisphere.

properties are based on the approach of Functionally Graded Material. Their through-the-thickness properties are to be based on layered composition of the wall thickness.

3 Functionally Graded Material, FGM

3.1 Background

The Functionally Graded Material, FGM, consists of a mixture of two different types of material – usually metal and ceramics. They are achieved by slowly changing the volume fraction of the constituent material. This approach proved to be successful in structural elements subjected to high temperature. The rule of mixtures has been used to estimate elastic properties of resulting composite materials by combining the properties of their individual components.

In our case we consider 'a mixture' of steel and auxetic materials. The effective material properties of FGM can be defined by the rule of mixtures (Voight model), as follows:

$$F = F_s V_s + F_a V_a \tag{1}$$

where V_s and V_a are the volume fractions of the steel and auxetic, respectively. They are related by:

$$V_a + V_s = 1 \tag{2}$$

It is customary to assume that the volume fraction V_a can follow one of the following power laws:

1. Linear:

$$V_a = \bar{z} + 0.5 \tag{3}$$

2. Quadratic:

$$V_a = (\bar{z} + 0.5)^2 \tag{4}$$

3. Inverse quadratic:

$$V_a = 1 - (0.5 - \bar{z})^2 \tag{5}$$

4. Cubic:

$$V_a = 3(\bar{z} + 0.5)^2 - 2(\bar{z} + 0.5)^3 \tag{6}$$

The variation of the auxetic volume fraction through the thickness of FGM shell is shown in figure 5a, where $\bar{z} = \frac{z}{t/2}$, with variable $'z'$ indicating the position along the thickness of FGM shell, i.e., $-0.5 \leq z \leq +0.5$
From Equations (2) and (4), the effective Young's modulus and Poisson's ratio of FGMs can be written as

$$E(\bar{z}) = (E_s - E_a)V_a + E_a\,, \qquad \nu(\bar{z}) = (\nu_s - \nu_a)V_a + \nu_a \tag{7}$$

where E_a, ν_a, E_s, ν_s are theYoung's modulus and Poisson's ratio of the auxetic and steel surfaces of the FGM shell, respectively.
Out of four possible rules of mixture given by Equations (3–6) the inverse quadratic power law, Equation (5) is adopted in what follows. Figure 5a plots the change of volume fraction, V_a, as the dimensionless parameter. The ratio (2z/t), changes from 2z/t = -0.5 to 2z/t = +0.5. The other distributions listed above do not differ in any significant manner.

3.2 Modelling details and results

The following values were taken for modelling continuous, through the thickness properties. The Young's modulus of steel, E_s = 207.0 GPa, modulus of auxetic, E_a = 20.7 GPa. The Poisson's ratios were taken as, υ_s = +0.30, and υ_a = -0.90. Using the Equation (7) one could get the magnitudes of Young's modulus and Poisson's ratio for different point values going through the shell wall thickness. With reference to figure 3a, values of E and υ were computed for a string of initial (t_a/t_s)-ratio between 0.30 and 0.90. Plot of E and υ for the case of (t_a/t_s) = 0.45 is shown in figure 5b. The values, in the middle of layer no. 1 and no. 6, are marked by a large dot in this figure. For the analysis purpose, the wall thickness was divided into six layers of which the external layer no. 1 was from mild steel, and the remaining five were auxetics. The values given in Table 1 are for several magnitudes of (t_a/t_s)-ratio taken from the range $0.30 \leq (t_a/t_s) \leq 0.90$. They are given in the middle of each of six-layer wall thickness. This data facilitated stability analysis using Bosor5 software. The yield point for each layer was taken as, σ_{yp} = 300 MPa with elastic data taken from the FGM modelling.

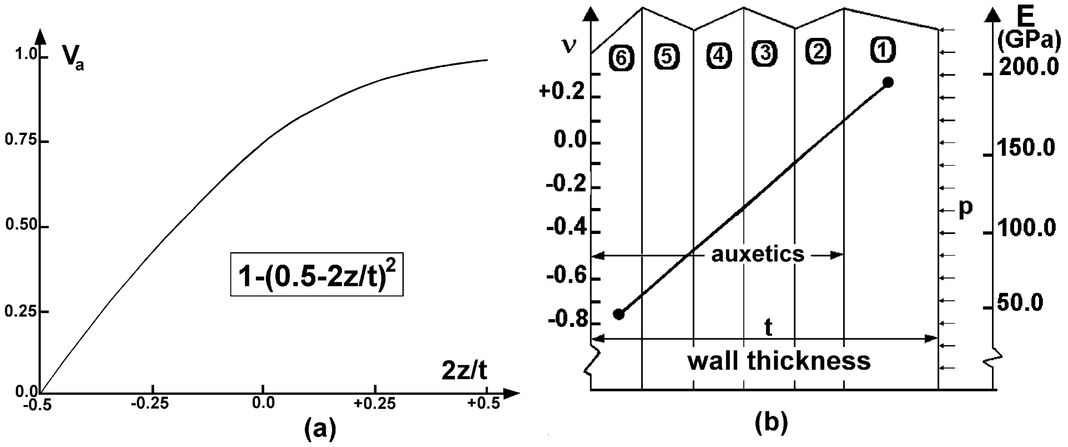

Figure 5: Plot of inverse quadratic volume fraction auxetic, V_a (Fig. 5a). Change of Poisson's ratio and Young's modulus in FGM wall thickness.

	t_a/t_s	0.30		0.45		0.55		0.70		0.90	
		υ	E	υ	E	υ	E	υ	E	υ	E
layer	1s	+0.15	184.2	+0.21	192.9	+0.24	197.6	+0.27	207.8	+0.30	206.5
	2a	-0.34	107.7	-0.13	141.1	-0.01	159.5	-0.18	133.1	-0.49	84.77
	3a	-0.45	90.73	-0.26	120.0	-0.15	136.5	-0.01	158.5	-0.18	133.1
	4a	-0.57	72.40	-0.42	95.10	-0.33	109.1	-0.21	128.3	-0.06	150.6
	5a	-0.69	52.73	-0.60	67.61	-0.54	77.11	-0.45	90.73	-0.34	107.7
	6a	-0.83	31.71	-0.79	37.09	-0.77	40.03	-0.74	45.9	-0.69	52.7

Table 1: Values of Poisson's ratio,υ, and Young's modulus, E, in the middle of layers 1 to 6. Note: E is given in thousands of MPa (e.g., 184200 MPa).

Elastic perfectly plastic analysis with nonlinear geometry was carried out. Results are plotted in figure 6. They are compared with results obtained for a two-layer torisphere of the same geometry, and 50% of the wall being steel ($\upsilon_s = +0.30$), and 50% of the wall thickness being auxetic ($\upsilon_a = -0.90$). It is seen here that there are two distinct ranges: (i) $0.80 \leq (t_a/t_s) \leq 1.0$, where FGM-shell has the larger magnitude of buckling pressure than two-layer shell by about 14%, and (ii) $0.30 \leq (t_a/t_s) < 0.80$ where the FGM shell is weaker than two-layer shell by about 15%. At the next stage the load deflection curves for 6-layer FGM and 2-layer torispheres were compared. In both cases apex deflection was measured for increasing magnitude of pressure for up to collapse. Results are depicted in figure 6. It is seen here that there is no difference, as both plots are near identical. The FGM-model bifurcates at pressure which is about 13% below the bifurcation load of geometrically identical 2-layer torisphere. From practical experience it is obvious that there is no post-bifurcation strength at all. Numerically though one can carry calculations well beyond the bifurcation load. The results are however irrelevant from practical point of view. Nevertheless, the calculations were carried out here for both FGM and 2-layer shells. It is seen from figure 6 that the collapse of the FGM model is some 23% above the collapse magnitude of 2-layer model.

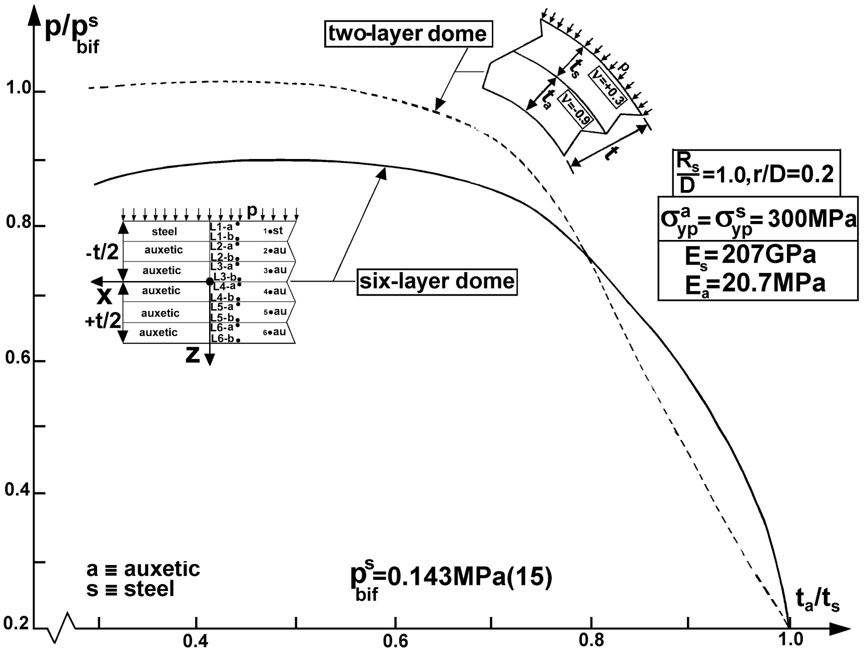

Figure 6: Comparison of buckling pressure of two-layer with 6-layer FGM torispheres.

One of important features of layered shells is the discontinuity of stresses between two neighbouring layers. These were extracted at bifurcation loads for FGM-shell (p_{bif} = 0.129 MPa, n = 16), and for geometrically identical 2-layer shell (p_{bif} = 0.146 MPa, n = 16). Results for the FGM-torisphere are given in Table 2. The jump of effective stresses between inner layers changes from 0.94 to 1.08. At the same time the jump between top surface of steel layer and bottom surface of the last auxetic layer was 2.23. The results, at bifurcation, for two-layer head were: top/bottom surfaces 15.0, and the jump between two layers was equal to 16.0.

layers	surfaces of stress jump	ratio of jump
L1/L6	$L1-a/L6-b$	2.23
L1/L2	$L1-b/L2-a$	1.08
L2/L3	$L2-b/L3-a$	1.05
L3/L4	$L3-b/L4-a$	1.0
L4/L5	$L4-b/L5-a$	1.0
L5/L6	$L5-b/L6-a$	0.94

Table 2: Ratio of effective stresses at top/bottom surfaces (L1-a ≡ steel layer, top surface; L6-b ≡ auxetic layer, bottom surface). Also, ratio of effective stresses between bottom ('b') and top ('a') layers. Values recorded at maximum stresses located at s_{max}/s_{total} = 0.66 from apex.

4 Closure

Recent development of a seamless auxetic substrate film capable of integrating porous auxetic layers has motivated this study. It showed that a six-layer torisphere with graded properties has in some instances larger magnitudes of buckling pressure than geometrically equivalent shell. These gains spread over a sizeable range of (t_a/t_s)-ratio, especially where the contribution of 'auxetic thickness' is close to 100%. In other investigated area (with the diminished contribution of auxetic thickness), the magnitude of buckling pressure in equivalent domes is smaller than in two-layer heads. As expected, the magnitude of stress jump between inner layers is nearly non-existent. The jump between top and bottom surfaces is significantly smaller than the one in two-layer dome.

These results are obtained for thin shells with the same yield point of material. It would be advisable to generate slowly varying magnitude of the yield and add it to Functionally Graded Material philosophy.

Finally, it has to be said that translating the current laboratory successes (including scaling-up), into commercially viable structural elements will define their success/demise in the long term.

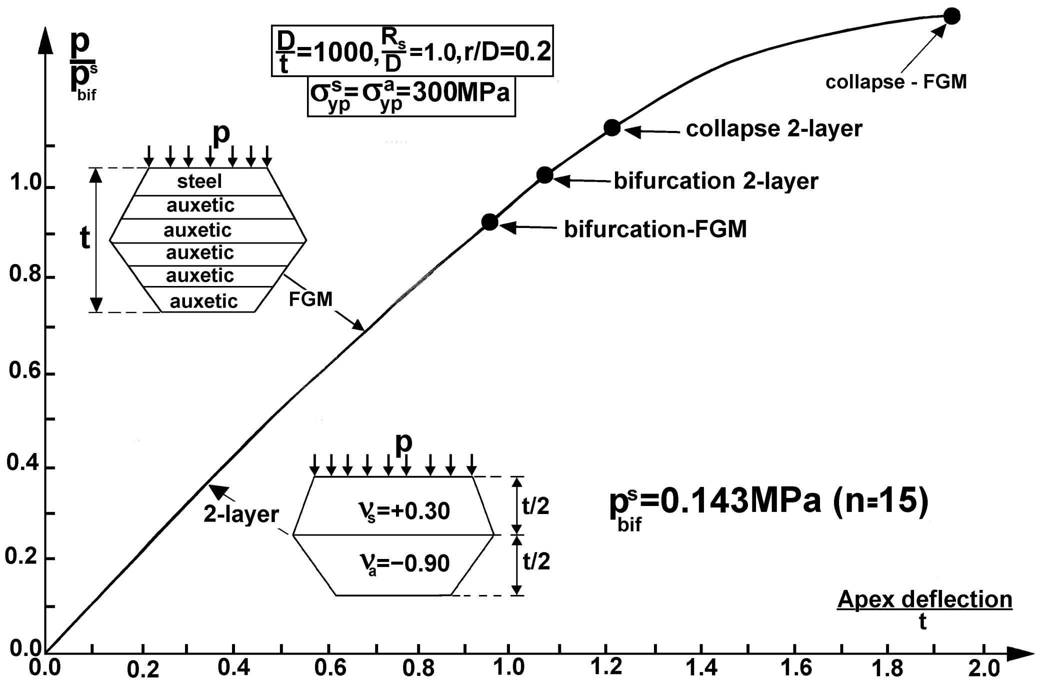

Figure 7: Load-deflection curves for 2-layer and six-layer FGM torisphere (the case (t_a/t_s) = 0.55). Also, E_s = 207.0 GPa and E_a = 20.70 GPa.

References

[1] J. Singer, J. Arbocz, T. Weller, "Buckling experiments – Experimental Methods in Buckling of Thin-Walled Structures", Volume 2, 2002, John Wiley & Sons, NY, USA, 1732 p., (ISBN 0-471-9.450-1).

[2] J. Błachut, "Experimental perspective on the buckling of pressure vessel components". Applied Mechanics Reviews, Transactions of the ASME, 66, 2014, 010803-1 – 010803-24.

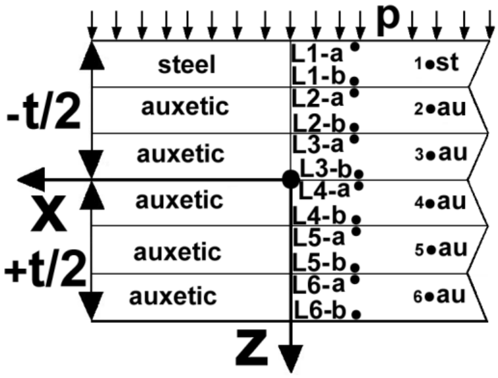

Figure 8: Section through the wall thickness made from six-layers (one steel and five auxetic). Convention for surface stresses at the neighbouring layers.

[3] J. Zhang, M. Zhang, W.C. Cui, W.X. Tang, F. Wang, B.B. Pan, "Elastic-plastic buckling of deep sea spherical pressure hulls", Marine Structures, 57, 2018, 38-51.

[4] H. Wagner, C. Huhne, J. Zhang, W. Tang, "On the imperfection sensitivity and design of spherical domes under external pressure", Intl Journal of Pressure Vessels and Piping, 179, 2020, 104015, 1-12.

[5] NASA, "Buckling of Thin-Walled Doubly Curved Shells", NASA, Space Vehicle Design Criteria (Structures), Report No. NASA SP-8032, 1969, pp. 1-33.

[6] ASME, "Alternative Rules for Determining Allowable External Pressure and Compressive Stresses for Cylinders, Cones, Sphere and Formed Heads, Section VIII, Divisions 1 and 2", Cases of the ASME Boiler and Pressure Vessel Code, American Society of Mechanical Engineers, New York, 2008, pp. 1-13, Standard No. Code Case 2286-2.

[7] ECCS TC8 TWG 8.4 Shells, Buckling of Steel Shells – European Design Recommendations, No. 125, 2013, 5th edition (revised), ECCS, Multicomp Lda, Portugal, (ISBN 978-92-9147-116-4), pp. 319-340.

[8] PD 5500, Public Document: "Specification of unfired fusion welded pressure vessels", British Standards Institution, London, 9th Edition, 2024.

[9] N. Yamamoto, R. Guzman de Villoria, B.L. Wardle, "Electrical and thermal property enhancement of fiber-reinforced polymer laminate composites through controlled implementation of multi-walled carbon nanotubes" Composites Science and Technology, 72, 2012, 2009-2015.

[10] M.A. Elezz, N.M. Aboeleneem, N.M. Abd-ElMonem, "A comprehensive review: Functional nanomaterials for renewable energy: Innovations, applications, and sustainable strategies", New Materials, 9, 2025, 10101-1 – 10101 – 20.

[11] Hibbitt, Karlsson, and Sorensen Inc., ABAQUS – Theory and Standard User's Manual Version 6.4, 2006, Pawtucket, RI, 02860-4847, USA.

[12] D. Bushnell, "Bosor5: program for buckling of elastic-plastic complex shells of revolution including large deflections and creep", Computers and Structures, 6, 1976, 221-239.

[13] J. Błachut, “Buckling behaviour of auxetic domes under external pressure”, Thin-Walled Structures, 2023, 182. 110262-1 – 110262-7.

[14] J. Błachut, G.D. Galletly, “Influence of local imperfections on the collapse strength of domed end closures”, Proceedings of the Institution of Mechanical Engineers Part C – Journal of Mechanical Science, 1993, 207(3), 197-207.

[15] Y. Zhou, D. Jiang, L. Wang, P. Xiang, L-J. Jia, “Cushioning performance of origami negative Poisson’s ratio honeycomb steel structure”, Thin-Walled Structures, 204, 2024, 112284, 1-13.

[16] Ch. Mercer, T. Speck, J. Lee, D.S. Balint, M. Thielen “Effects of geometry and boundary constraint on the stiffness and negative Poisson's ratio behaviour of auxetic metamaterials under quasi-static and impact loading”, International Journal of Impact Engineering, 169, 2022, 104315, 1-12.

[17] P.T. Thang, Ch. Kim, H. Jang, T. Kim, J. Kim, “Buckling behaviour analysis of hybrid-honeycomb sandwich cylindrical shells”, Ocean Engineering, 276, 2023, 114214, 1–12.

[18] V. Siniauskaya, H. Wang, Y. Liu, Y. Chen, M. Zhuravkov, Y. Lyu, “A review on the auxetic mechanical metamaterials and their applications in the field of applied engineering”, Frontiers in Materials, 11(August), 2024, 1-14, (doi: 10.3389/fmats.2024.1453905).

[19] J. Błachut, “Buckling behaviour of auxetic domes under external pressure”, Thin-Walled Structures, 182, 2023, 110261, 1-7.

[20] J. Błachut, D. Sala, “Externally pressurized auxetic domes – buckling performance”, Proceedings of the Thirty-third International Ocean and Polar Engineering Conference, ISOPE-2023, Ottawa, June 19-23, 2023, 3893-3897, ISSN 1098-6189.

[21] J. Błachut, M.D. White, “Elastic-plastic buckling of externally pressurized auxetic domes”, Thin-Walled Structures, 214, 2025, 113324, 1-13.

[22] J. Blachut, M.D. White, “Influence of material and shape imperfections on buckling of externally pressurised auxetic domes”, in Proc. of the Eighteenth Intl Conf. on Civil, Structural and Environmental Engineering Computing, (eds) P. Ivanyi, J. Kruis, and B.H. Topping, vol. 10, paper 13.1, Cagliari/Sardinia, August, 2025 (doi:10.4203/ccc.10.13.1).

[23] Y. Lee, B. Jang, H. Song, S. Kim, Y. W. Kwon, H.S. Kang, M.S. Kim, I. Park, T-S. Kim, J. Jang, J-H. Kim, J-U. Park, B-S. Bae, “A seamless auxetic substrate with a negative Poisson’s ratio of -1”, Nature Communications, 15, 2024, 7146, pp 1-9, (https://doi.org/10.1038/s41467-024-51516-1).

[24] A.H. Sofiyev, N. Kuruoglu, M. Turkmen, “Buckling of FGM hybrid truncated conical shells subjected hydrostatic pressure”, Thin-Walled Structures, 47. 2009, 61-72.